

Abstract

Recently several studies paved a way to nearly 100% selectivity of the electrochemical ammonia synthesis (EAS), which had been identified earlier as a main challenge. These results motivated us to benchmark the energy efficiency (EE) of EAS against the Haber-Bosch process. We present a method to calculate EE of EAS, which can be used by a broader audience. EAS studies historically suffered from reliability issues, and to avoid benchmarking of false-positive results, we established a method to calculate a reliability indicator to assess the measurement reliability of a published work. We used the indicator to evaluate the studies published in 2020, 2021 and 2022. We calculated the EE of EAS for works that were assessed as reliable with our indicator. We identified and discussed several promising systems and strategies enabling higher selectivity and EE. The EE of some aqueous EAS reports are up to 55%, and non-aqueous are below 15%.

Low-temperature electrochemical ammonia synthesis: measurement reliability and comparison to Haber-Bosch in terms of energy efficiency

Fateme Rezaie¹, Søren Læsaa¹, Nihat Ege Sahin¹, Jacopo Catalano,¹ Emil Drazevic^{1,*}

Fateme Rezaie (frezaie@bce.au.dk), Søren Læsaa (laesaa@bce.au.dk), Nihat Ege Sahin

(nsahin@bce.au.dk), Jacopo Catalano (jcatalano@au.dk), Emil Drazevic (edrazevic@bce.au.dk)

¹Aarhus University, Department of Biological and Chemical Engineering, Aabogade 40, 8200 Aarhus N, Denmark

Introduction

Green ammonia can be produced using a Haber-Bosch process combined with a renewable-energy-powered electrolyser as a source of green hydrogen. Green hydrogen and dinitrogen separated from air are reacted to form green liquid anhydrous ammonia. Here adjective “green” means ammonia is produced in a sustainable way. This process is energy efficient and proceeds at high pressures (150-300 bar) and high temperatures (350-520 °C).¹ The Haber-Bosch process is highly optimized for large-scale production, where high capital costs are justified by large volumes of ammonia production during the plant lifetime. But the process is not suitable for small scales of production (< 1 ton/h) and cannot address all market needs, mainly because heat-exchangers and compressors make up to 50% of the capital cost and this cost cannot be justified at smaller scales.²

Low-temperature (room temperature) electrochemical synthesis of green ammonia appears as a promising alternative to the green Haber-Bosch process. The reaction is performed in an electrochemical reactor at lower temperatures and pressures³, without the need for costly components for heat recovery and for withstanding high pressures.⁴ Operating at lower temperatures and milder pressures could help reduce capital costs, making the process relevant for smaller scales.⁵ The electrochemical route has potential for decentralized production of ammonia⁶ e.g., in vertical farming or at remote locations where transport costs make up a significant share of the total ammonia cost.

There have been several breakthroughs in this field, where Electrochemical Nitrogen Reduction Reaction (ENRR) was engineered to occur at near to 100% selectivity, and this field is no longer challenged by selectivity issues, as it historically was.⁷ High selectivity of ENRR

has been reported in both aqueous and non-aqueous media. Furthermore, new start-up companies intending to bring these technologies to the market have been established, and with these recent developments it is timely to assess electrochemical synthesis of ammonia for energy consumption and efficiency and benchmark it against the well-known Haber-Bosch Process.

Until very recently ENRR was challenged by selectivity where proton or water reduction to hydrogen occurred predominantly as a side reaction.^{8,9} Hydrogen evolution reaction (HER) is kinetically favoured, as it occurs in fewer steps than ENRR. Additionally, ENRR is often performed in aqueous media, where the solubility of N₂ is only about 0.7 mM at room temperatures and atmospheric pressure, while the concentration of the competing reactant that is involved in HER, i.e. water, is around 55 M, tens of thousands times more. The rates of electrochemical ammonia production in aqueous media are therefore often very low.

Because of low ENRR ammonia production rates, contamination can have a significant impact on an experimental result and lead to false positive measurements. For instance, ammonia was found present in the air, human breath, adsorbed within ion-exchange membranes as well as in nitrogen feed gas.¹⁰ The presence of oxidized forms of nitrogen (NO_x), such as nitrate anions in catalyst materials, electrolytes for electrochemical cells, laboratory gloves and glassware and nitrogen oxides in nitrogen gas supplies or air, was also found problematic, because oxidized forms of N are more soluble in water and thermodynamically and kinetically easier to reduce to ammonia than dinitrogen, which highlights the need to properly clean the gases.^{6,11,12} Some recent results reveal that some metal nitrides undergo chemical decomposition to produce ammonium instead of catalysing ENRR, which is yet another way of having a false positive measurement.¹³

To address the above-reported concerns, we developed a new methodology that allowed us to calculate a reliability indicator of ENRR measurement. Earlier attempts exist in the literature, however not in the form presented in this article.¹⁴ Our methodology is established from rigorous ENRR protocols,¹⁰ proposed by the research community to unambiguously confirm ENRR and stimulate the progress in the field.^{12,13} We used the reliability indicator to assess the reliability of the articles. We assessed 456 ENRR works indexed in Web Of Science and published in 2020, 2021 and 2022, using keywords electrochemical ammonia synthesis. Reliability indicator helped us focus the discussion of this research on the most promising catalysts, electrolytes, membranes, and cell designs. We propose a simple method to calculate

the energy efficiency of ENRR works, that allows for benchmarking of ENRR against Haber-Bosch process. We calculated energy efficiency of most promising ENRR approaches and benchmarked them against the Haber-Bosch process. The energy efficiency we calculated should be considered as an upper bound.

Methods

A method to calculate the reliability indicator

We evaluated each study in terms of two criteria: *experimental controls* and *ammonia production rate*. The outputs of this step allowed us to establish a reliability indicator table and calculate a reliability indicator to assess how likely the measurement was a false positive, as elaborated in more details below. At the onset, we emphasize that the reliability indicator is just a numerical index, the only purpose of which is to fulfil the function of indicating if a measurement is reliable or probably not reliable. For a more definite assessment of the measurement reliability, the work needs to be experimentally reproduced, including synthesis of the catalyst and electrochemical tests.

The methodology we used to assess the measurement reliability of ENRR articles is depicted in Fig. 1.

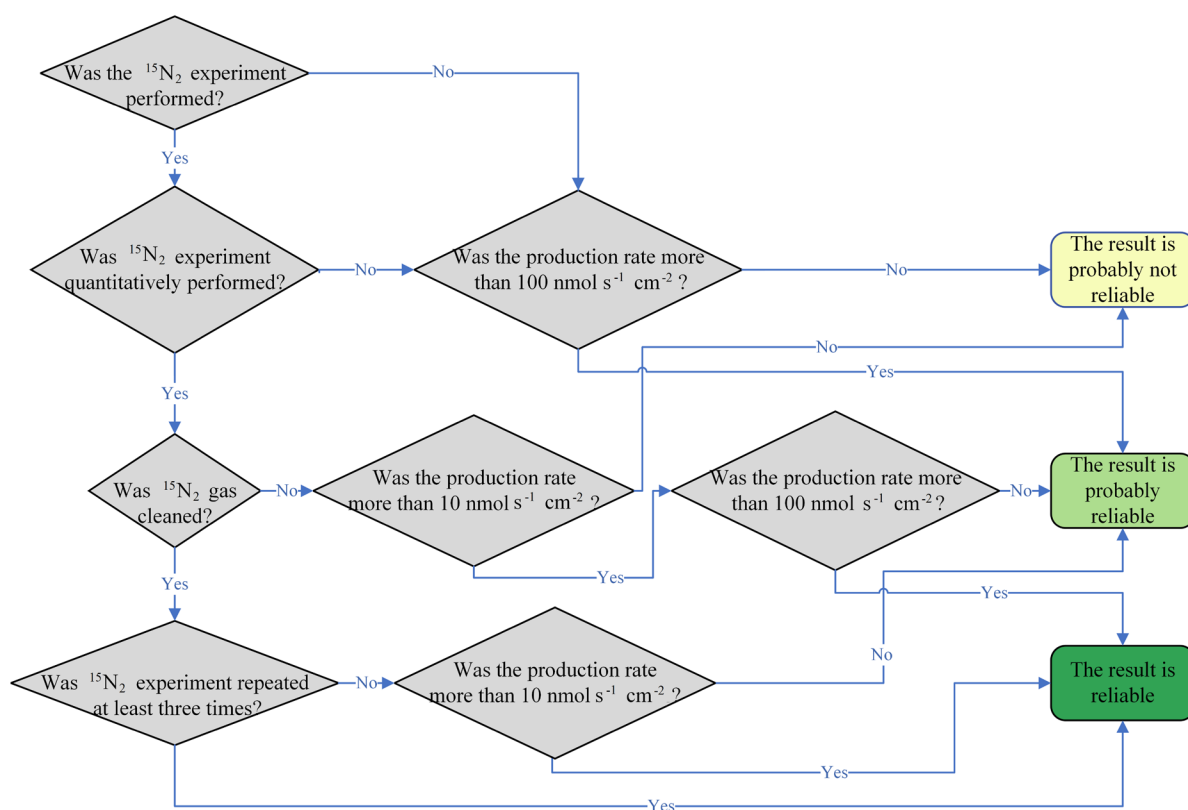


Figure 1 – Experimental protocol requirements to avoid false positive results and deliver reliable outputs: this flowchart is used to assess the articles and determine their reliability.

Experimental controls are a necessity to confirm the ENRR and to advance the state of the art of the ENRR field. We reviewed ENRR experimental protocols (SI section 1) to identify the requirements needed to unambiguously confirm the ENRR.

Based on the review of experimental protocols, the claim that ammonia stems from ENRR was very likely if: i) the amount of ammonia produced with $^{14}\text{N}_2$ is quantitatively reproducible with the $^{15}\text{N}_2$ experiments, ii) the gases have been adequately cleaned, and iii) the experiments were performed at least in triplicate and shown to be repeatable.

Scoring of the experimental control. To evaluate the works based on the experimental control criterion, we have adopted the scale presented in Table 1, where the highest number defines the most reliable measurement. There is a smaller chance that the ammonia stemmed from a contamination of purified gas. Here we put more weight on those experiments that did the nitrogen isotope tests, cleaned all gases (including isotope) and repeated the experiments. For this purpose, we used a sigmoid-shaped function to score the intervals, as shown in Table 1. Here the plateau was sat 25, for works that performed three or more $^{15}\text{N}_2$ experiments with clean gases.

Table 1 – Sigmoid-shaped scored confidence intervals of different types of experiments performed in ENRR works.

Experimental control	Scale
No $^{15}\text{N}_2$ experiment	1
Qualitative $^{15}\text{N}_2$ experiment, without gas cleaning or repeating the experiment	2
Quantitative $^{15}\text{N}_2$ experiment, without gas cleaning or repeating the experiment	3
Quantitative $^{15}\text{N}_2$ experiment, with gas cleaning, but without repeating the experiment	10
Quantitative $^{15}\text{N}_2$ experiment, with gas cleaning and repeating the experiment	25

Ammonia (J_{NH_3}) production rate is a measure of the reliability of the measurement. If the rates were low, it would have been difficult to discern between the ammonia stemming from contamination and actual production stemming from ENRR.¹⁴ However, if ammonia production rates were high, the amount of produced ammonia would have been much higher than the contamination levels, which indicates a more reliable result.

Scoring of the ammonia production rate (J_{NH_3}). The minimum acceptable practical ammonia production rate for electrochemical ammonia synthesis was established as $100 \text{ nmol s}^{-1} \text{ cm}^{-2}$.¹⁵ In our evaluation of this criterion, we used the scale presented in Table 2. The scales are derived from Choi et al.'s work¹⁴ where ammonia production rates are divided in four tiers. The scoring of the intervals follows a quasi-logarithmic scale covering more than three orders of magnitudes, and it plateaus at 10. Here, the lowest production rate level (below $0.1 \text{ nmol s}^{-1} \text{ cm}^{-2}$) has the lowest score of 1, while the highest has a score of 10. If production rates are higher than $100 \text{ nmol s}^{-1} \text{ cm}^{-2}$ ENRR works would be considered competitive with the Haber-Bosch process and this is yet another reason to mark it high.

Table 2 – Quasi-logarithmic shaped scored intervals of ammonia production rate reported in various ENRR works.

Ammonia production rate	Scale
Ammonia production rate $< 0.1 \text{ nmol s}^{-1} \text{ cm}^{-2}$	1
$0.1 < \text{Ammonia production rate} < 10 \text{ nmol s}^{-1} \text{ cm}^{-2}$	2
$10 < \text{Ammonia production rate} < 100 \text{ nmol s}^{-1} \text{ cm}^{-2}$	4
Ammonia production rate $> 100 \text{ nmol s}^{-1} \text{ cm}^{-2}$	10

The reliability indicator. To determine the reliability of the measurement, we multiplied the scale values from Table 1 and Table 2 to calculate a new value, that we named the reliability indicator. The reliability indicator is presented as a matrix in Table 3. We defined three levels of confidence based on reliability indicator: dark green, green, and light green, representing “reliable”, “probably reliable”, and “probably not reliable”, respectively. The boundaries were carefully chosen as 10 and 25 to divide the articles into three levels of reliability. More specifically, we assign a high weight for a well-performed $^{15}\text{N}_2$ experimental control. For example, the first boundary index, 10, is the product of “quantitative $^{15}\text{N}_2$ experiment, with gas cleaning, but without repeating the experiment” and an unlikely practical production rate

($J_{NH_3} < 0.1$), which means even with a very low production rate and no repeatability, the result is probably reliable. The next boundary index is 25 because it results from a highly reliable $^{15}N_2$ experimental control that did the gas cleaning and repeated the experiments, however reporting a low production rate ($J_{NH_3} < 0.1$). Finally, we score 250 for a work with practically relevant production rate and highly reliable $^{15}N_2$ experimental control that considered the gas cleaning and repeated the experiments.

Table 3 - Reliability indicator matrix – In this matrix, two intervals (10 and 25) were used to divide the reliability indicator into three levels: reliable, probably reliable, and probably not reliable. If the reliability indicator value is less than 10 the work falls within a “probably not reliable” interval and is marked with light green colour. If the reliability indicator was between 10 and 25 the work falls within a “probably reliable” and is marked with green colour, and finally if the reliability indicator was greater than 25 the work falls within a “reliable” interval and is marked with dark green colour.

Reliability indicator		Ammonia production rate (nmol s ⁻¹ cm ⁻²)			
		$J_{NH_3} < 0.1$	$<J_{NH_3} < 10$	$J_{NH_3} < 100$	$J_{NH_3} > 100$
$^{15}N_2$ experimental controls	Scale	1	2	4	10
No $^{15}N_2$ experiment	1	1	2	4	10
Qualitative $^{15}N_2$ experiment, without gas cleaning or repeating the experiment	2	2	4	8	20
Quantitative $^{15}N_2$ experiment, without gas cleaning or repeating the experiment	3	3	6	12	30
Quantitative $^{15}N_2$ experiment, with gas cleaning, but without repeating the experiment	10	10	20	40	100
Quantitative $^{15}N_2$ experiment, with gas cleaning and repeating the experiment	25	25	50	100	250

Method to calculate the energy efficiency of ENRR works

Energy efficiency of ENRR. The energy efficiency of the ammonia synthesis process can be expressed as a power to fuel efficiency (η_{LHV}), which can be defined as:

$$\eta_{LHV} = \frac{LHV}{\Delta H_R} \quad (1)$$

where LHV is the lower heating value of ammonia (kJ/mol) and ΔH_R is the molar enthalpy of the reaction where fuel is synthesized (kJ/mol). In case of green ammonia, ΔH_R refers to the chemical reaction $\frac{1}{2} \text{N}_2(\text{g}) + \frac{3}{2} \text{H}_2\text{O}(\text{l}) \leftrightarrow \text{NH}_3(\text{g}) + \frac{3}{4} \text{O}_2(\text{g})$, where $\Delta H_R = 383$ kJ/mol, which is calculated from the products and reactants standard enthalpy of formation,¹⁶ as H_2 in green ammonia synthesis comes from water. The lower heating value (LHV) is the amount of energy released from burning 1 mol of fuel without recovery the latent heat of condensation of steam. LHV of ammonia is 317 kJ/mol¹⁷ and by using Eq. (1) we can calculate, in case of green ammonia synthesis from water as a source of hydrogen, the maximum attainable thermodynamic energy efficiency as $\eta_{LHV} = 82.77\%$. Practically, energy efficiency is calculated by dividing the LHV by the total energy input needed to synthesize ammonia, which includes the energy losses.

We calculated the energy needed to run the nitrogen electrolyser and used it as total energy input, meaning all energy efficiencies are overestimated, as elaborated in more details below. Electrical energy input to power up the nitrogen electrolyser is related to the working full cell voltage of an electrolyser, E_{cell} , which is defined as Eq. (2).

$$E_{\text{cell}} = E_{\text{ENRR}} - E_{\text{anode}} \quad (2)$$

where E_{anode} is the practically relevant potential at which water, hydrogen, or ethanol (depending on what is the source of the protons) gets oxidized. Eq. (2) does not contain any ohmic parasitic resistance (e.g. contact resistances, membrane resistance), and thus can be considered a lower limit for the operating voltage of a working device. E_{anode} is normally not reported; however, water oxidation potentials at different pH are readily available in the literature. For aqueous systems, we surveyed eight works and found the water oxidation potential (mean \pm standard deviation) to be 1.6 ± 0.17 V vs. RHE (section 2, Table S1). For ethanol-based systems 0.4 V vs. RHE is used.¹⁸ E_{ENRR} is the potential at which N_2 gets reduced to ammonia in a particular electrolyte, which is reported in ENRR works. E_{cell} calculated in Eq. (2) includes all the overpotentials and thus energy losses associated with the electrodes. The total electrical work used to power the electrolyser is given by Eq. (3):

$$W(\text{NH}_3) = \frac{-nNFE_{\text{cell}}}{F.E.} \quad (3)$$

where $W(\text{NH}_3)$ is the electrical work (kJ/mol), n is number of moles of ammonia, N is the number of electrons transferred per molecule of ammonia (which is 3), F represents Faraday's

constant, and $F.E.$ is Faraday efficiency. For aqueous systems the energy efficiency can be approximated as:

$$\eta_{\text{aq}} = \frac{LHV}{W(\text{NH}_3)} \quad (4)$$

Here $W(\text{NH}_3)$ in Eq. (4) is a close proxy for the total energy input since it does not account for heat (entropy) input. However, this latter contribution is low at 25 °C relatively to the $W(\text{NH}_3)$. We do not consider energy used to separate nitrogen from air, compress the gases and energy needed to separate clean liquid and anhydrous ammonia from the process. However, by doing so we still get a practically relevant information in how the process stands against Haber-Bosch as energy input in Eq (4) is assumed the largest (around 80%)

For anhydrous systems we recognise the relevance of Eq. (4) for reporting energy efficiency of a given setup. However, when comparing aqueous and non-aqueous systems one needs to account for the energy input of producing the proton and electron source. Anhydrous systems are usually “fuelled” by hydrogen or ethanol, and the energy used to produce these chemicals should be considered when comparing the energy efficiency. For hydrogen as proton and electron source, energy consumption can be calculated as energy used by alkaline electrolyser, where electrical work can be calculated with Eq. (5).

$$W(\text{H}_2) = \frac{-nN(\text{H}_2)FE_{\text{electrolyser}}}{F.E.} \quad (5)$$

Where $N(\text{H}_2) = 3$ electrons ($3/2 \text{ H}_2$ react with $1/2 \text{ N}_2$ to form 1 mol NH_3), and $E_{\text{electrolyser}}$ is operating voltage of an alkaline electrolyser on a system level. Based on this equation, the energy needed to produce hydrogen is 707.56 kJ/mol NH_3 (see SI, section 4.1). The energy contribution from ethanol is estimated as 927.38 kJ/mol NH_3 (see SI, section 4.2).

For non-aqueous systems that used hydrogen gas or ethanol as a proton and electron source, the energy efficiency was calculated as described in Eq. (6) for H_2 and ethanol in Eq. (7).

$$\eta_{\text{non-aq}(\text{H}_2)} = \frac{LHV}{W(\text{NH}_3) + W(\text{H}_2)} \quad (6)$$

$$\eta_{\text{non-aq}(\text{EtOH})} = \frac{LHV}{W(\text{NH}_3) + \frac{3}{4} \times LHV_{\text{EtOH}}} \quad (7)$$

Here Eq. (3) was used to calculate $W(\text{NH}_3)$ and an estimate of E_{anode} in non-aqueous media was needed. In anhydrous systems where hydrogen was used at the anode, E_{anode} was set to 0.05 V vs. RHE.¹⁹ For ethanol-based systems 0.4 V vs. RHE was used.¹⁸ The real cell potential would be to some extent larger in a fully assembled electrochemical cell.⁴ More reliable estimates for

the electrical energy losses in a working device, need information from scaled up electrochemical stacks, which are not available as of today due to the TRL of this novel technology. In any case, the use of Eqs. (3)-(7) allows for a fair comparison of different ENRR systems as well as a preliminary comparison versus Haber-Bosh.

Energy efficiency of conventional Haber-Bosch plants ranges from 36 to 62% depending on the age of the plant and the technology provider.²⁰ The energy efficiency of the green Haber-Bosch process that couples the hydrogen production from water electrolysis with the thermocatalytic step used in the Haber-Bosch process is reported as 56%.¹⁶ We assumed ENRR must be run at least in this range of energy efficiencies to be competitive with Haber-Bosch. It is probably not realistic to expect energy efficiencies much higher than 60% in any ammonia-producing process, as the energy most intensive step in the Haber-Bosch process, which accounts for more than 90% of the energy use, is the hydrogen production where it proved very challenging to bring the energy cost down. Indeed, hydrogen production always occurs with inherent energy losses, whether it is produced by electrolysis or steam reforming of methane or coal.²¹

To evaluate energy efficiency, we used the intervals presented in Table 4. If a probably reliable/reliable ENRR work had $\eta < 20\%$, the work was not considered practically relevant, because less than 1 out of 5 Joules of total used energy goes in ammonia production. In such cases, most of the energy is used to generate heat or produce by-product hydrogen. However, there can still be some niche markets where this energy cost is acceptable. If $20\% < \eta < 35\%$, the process was considered practically relevant in some applications where low capital cost might be more important than higher energy costs. The ENRR works in this range were identified promising, nonetheless they still need improvement. If the energy efficiency is in the range of $35\% < \eta < 60\%$, which was identified as the current range of efficiencies of Haber-Bosch ammonia plants, it was marked practically relevant. Finally, energy efficiencies higher than 60% were highly relevant and a future target not only for ENRR but also Haber-Bosch.

Table 4 – Classification of ENRR energy efficiency: the practically relevant of ENRR are classified into four different levels in terms of the energy efficiency

ENRR energy efficiency	Practically relevant level
$\eta < 20\%$	not practically relevant but still depends to target market

$20\% < \eta < 35\%$	probably practical relevant
$35\% < \eta < 60\%$	practically relevant
$\eta > 60\%$	highly relevant and future target

Results and discussion

The results of assessment with the reliability indicator

We assessed 456 articles indexed in Web Of Science in 2020, 2021 and 2022 and scored them with the reliability indicator. All the works we assessed are found in the SI, section 3. Tables S2, S3 and S4 show that a small fraction of works performed experimental controls in accordance with protocols, only about 3% (with a reliability indicator ≥ 25). The assessment of reliability of 456 articles reporting ENRR in aqueous and non-aqueous media resulted with 77 publications being probably reliable and rated green, as presented in Table S1, S2, and S3, and 21 publications rated dark green. This is illustrated in Fig. 2.

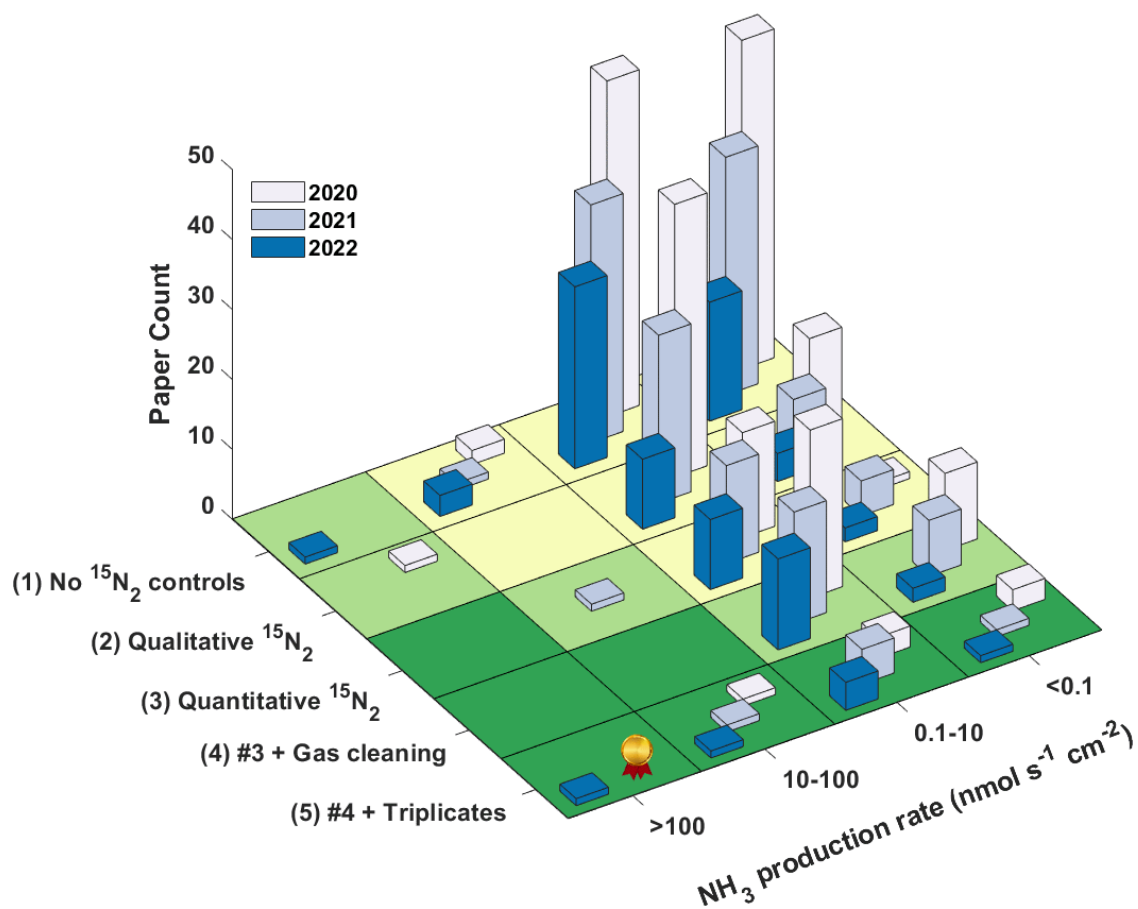


Figure 2- The distribution of the total number of the articles based on their score as a function of the reliability indicator. Dark blue refers to 2022, lighter blue to 2021 and light blue to 2020. Colour codes are taken from the Fig. 1. Scores are detailed in Table 3.

To preliminary examine how well can the reliability indicator indicate the measurement reliability, we identified three peer-reviewed studies we scored with the reliability indicator and that other researchers had attempted to reproduce experimentally.

Izellar et al.²² critically assessed the ENRR activity of molybdenum and iron carbides, trying to reproduce peer-reviewed works that had reported a superior or excellent catalytic performance.^{23,24} They found that the ammonia did not originate from the ENRR but from unavoidable extraneous ammonia and NO_x impurities. We scored the reports on molybdenum and iron carbides^{23,24} (those which have been published the period of 2020-2022) with the reliability indicators of 1 (articles number 54 and 79 in Table S1) and assessed them as probably not reliable.

Hanifpour et al.²⁵ investigated catalytic activity of niobium oxynitrides towards ENRR in an aqueous electrolyte at ambient conditions as a peer-reviewed work had claimed.²⁶ They found no sign of catalytically produced ammonia. We assessed the same article²⁶ Hanifpour et al. had assessed experimentally as probably not reliable with reliability indicator of 6 (article number 120 in SI, Table S3).

The above preliminary investigation implies the reliability indicator gives a good indication if the published work is reliable. But the indicator by no means can be used alone to state the result is not reliable. It can indicate the result is *probably not reliable*. To be able to state the result is *not reliable* the published study needs to be assessed experimentally.

In the next section, we focused the discussion on reports that were assessed as reliable with the reliability indicator.

Successful approaches for achieving the high selectivity of the ENRR

The selectivity of the ENRR measured through Faradaic efficiency spans from 0.35 to 99%, depending on the catalyst, electrolyte and the solvent (see Fig. 3). Until recently, the major problem associated with ENRR was very low selectivity toward NH₃, where most of the electrons and protons were involved in HER thereby producing hydrogen instead of ammonia.

The selectivity issue has been solved for both non-aqueous and aqueous media, which both demonstrate high selectivity (Fig. 3).

High selectivity of the reaction and high production rates was so far demonstrated only in non-aqueous, water-free, highly concentrated electrolytes with low proton concentration and a catalyst that strongly binds nitrogen, as elaborated in more details below.

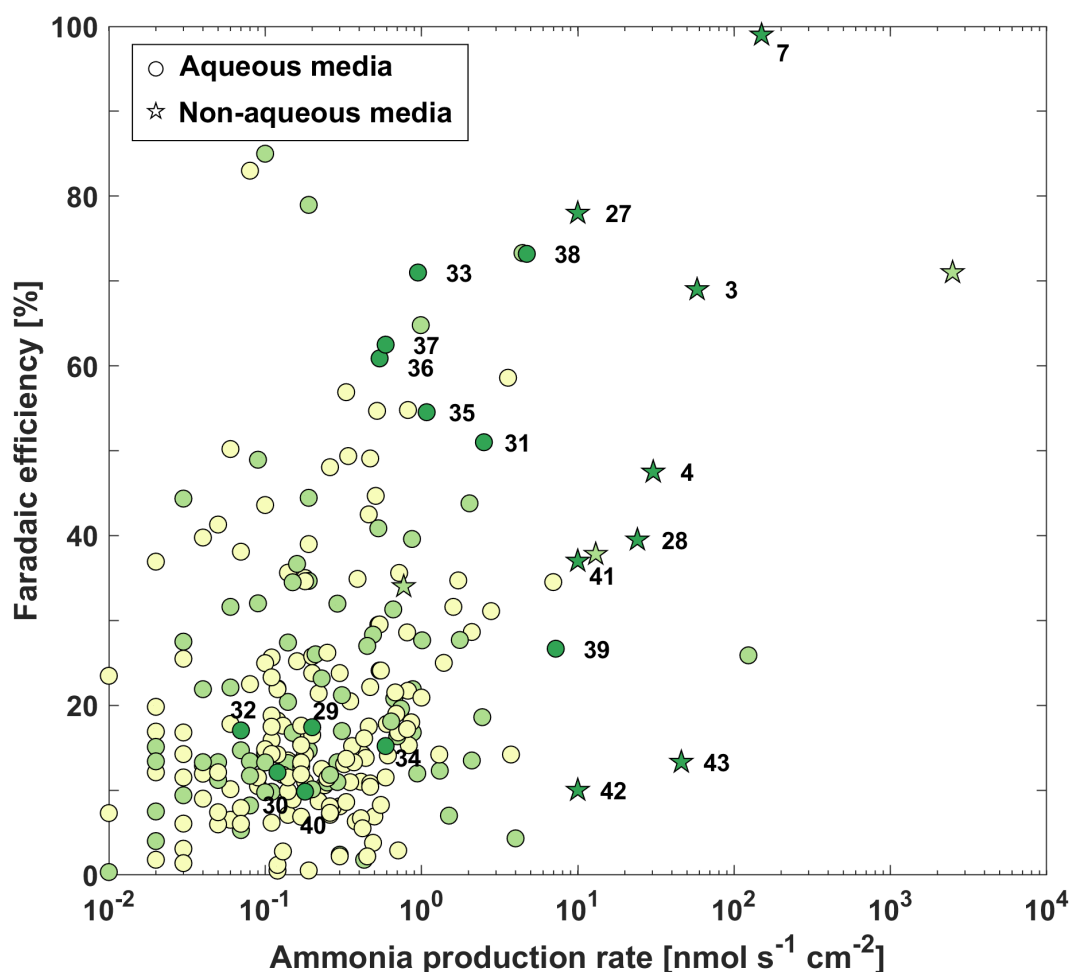


Figure 3- Reliability distribution of reviewed studies in terms of Faradaic efficiency – the dark green articles are reliable works, the green articles are probably reliable, and the light green articles are probably non-reliable, assessed using the methodology depicted in Fig 1 and specified in Table 3. Figure plots works that did isotope tests and these are found in SI, Section 3. ^{3,4,7,25,27-43}

Non-aqueous ENRR. The non-aqueous media-based reports are presented in SI, Table S4. All non-aqueous media reports are based on lithium-mediated electrochemical nitrogen reduction reaction (Li-ENRR). Non-aqueous works are found in the right side of the plot (Fig. 3), demonstrating much higher ammonia production rates than aqueous works, even if the Faradaic efficiency is in the same range of the aqueous works. This is in some part because the pressures of N₂ (up to 20 bar) are much higher than in aqueous works (mostly atmospheric pressure) and

in some part attributed to the fact that N_2 solubility in aqueous solutions is lower than in non-aqueous electrolytes, such as ionic liquids.⁴⁴ Higher N_2 solubility in electrolytes results in larger adsorption of N_2 at active catalyst sites.⁴⁴ Back in 2017, Singh et al.⁹ predicted that the selectivity challenge might be solved by reducing the proton concentration and using a catalyst that strongly binds nitrogen. They observed that NH_3 formation rate is zeroth order in the proton and electron concentration, while the H_2 formation rate is first order in both. Therefore, they concluded that a strategy for increasing the NH_3 selectivity could be to lower the accessibility of electrons, protons, or both. This would slow HER while the ammonia synthesis rate would be kept nearly the same. Based on this analysis, they proposed possible approaches to improve NH_3 selectivity might be in: i) decreasing the proton concentration in the electrolyte; ii) increasing the barrier for proton to transfer to catalyst surface in order to limit the proton transfer rate; iii) creating a thin insulating layer electrons must tunnel through or using photoabsorbers to supply a low flow of electrons in order to limit the electron transfer rate.⁹ Indeed reported works achieved high selectivity using one of the strategies explained above. Suryanto and coworkers³ implemented Li-ENRR for a reasonable time frame. They mentioned that one factor limiting the performance and longevity of the Li-ENRR system is the chemical nature of the proton source participating in reaction, which is mostly ethanol, and it is used as a sacrificial material somewhat implying there is an optimal acidity of the electrolyte. Indeed, this has been known earlier both on a theoretical and experimental level.⁴⁵ Therefore, they introduced a phosphonium salt as a genuine recycling proton shuttle that was electrochemically stable as there was a minimal tendency for it to be oxidised or reduced at the electrodes and has an optimal acidity constant (pK_a around 4). They pressurized their cell to 19.5 bar of nitrogen, and this enabled a high ammonia production rate at 69% Faradaic efficiency in 20-hour experiments. Furthermore, Li et al.²⁷ showed that adding a small amount of oxygen to the feed gas had a positive effect on the process that significantly improved the Faradaic efficiency up to 78% at 0.6 to 0.8 mole % oxygen in 20 bar of nitrogen and improved the stability of the system.

Cai et al.²⁸ applied the strategy of keeping deposited lithium fresh by increasing electrolysis current to increase ammonia yield rate and Faradaic efficiency up to 39.5%. They demonstrated that Li-ENRR began with electrochemical deposition of lithium, followed by two chemical reactions of dinitrogen splitting and protonation. So, the only dominant electrochemical process was lithium plating; therefore, the generation speed of new lithium could be easily

tuned by current. They also mentioned that fresh lithium could be obtained by retarding metallic lithium's passivation, which resulted from reaction between metallic lithium and electrolyte.

A breakthrough in Faradaic efficiency of nearly 100% was recently achieved by Du and coworkers.⁷ They investigated the role of electrolytes in Li-ENRR and presented a high Faradaic efficiency, approaching 100% at 15 bar nitrogen pressure. In this work, the electrolyte was high concentration imide-based lithium salt, making a compact ionic layering in the electrode-electrolyte interface. Several experiments were conducted to determine the optimum electrolyte type and concentration, as well as potential. LiNTf₂ was determined to be the best electrolyte among LiOTf, LiClO₄ and LiBF₄, and FSI⁻, with 2 M concentration at -0.55 V vs Li^{0/+}_{app}.

On a higher technology readiness level, Lazouski and coworkers⁴ used stainless steel cloth-based (SSCs) support as cathode and anode support to overcome hydrogen and nitrogen gas diffusion limitation of Li-mediated ENRR, respectively. They electrodeposited platinum onto the SSCs to be used as anode, as stainless steel is a poor hydrogen oxidation catalyst, and lithium metal was plated in situ onto SSC substrate applied as cathode. Despite the high Faradaic efficiency of 47.5% at ambient conditions, the cell potential was high 20-30 V, and the system was only stable for a short time. High voltages mainly arise from a very large electrical resistance of the non-aqueous electrolyte.

Aqueous ENRR. Seven aqueous works with Faradaic efficiency above 20% that were assessed as reliable with the reliability indicator are summarized in Table 5. The seven aqueous media-based ENRR were conducted in a membrane-separated two-compartment cell under ambient conditions, in which the membrane was either proton-exchange or microporous (Nafion 211,³⁷ Celgard,^{33,35} Nafion 117^{31,36,38,39}). The working electrode was a carbon paper^{33,35} or a carbon cloth^{36,37} deposited with catalyst or fabricated by coating the catalyst to a glassy carbon disc^{31,38,39}. Indeed, gas diffusion electrodes (GDEs) can be used to overcome the diffusion limitations of gaseous reactants in electrochemical reactions, enabling intimate contact between the gas, electrolyte, and catalyst. With GDEs, the distance that gas must travel through

the electrolyte to react at the catalyst surface is minimised, and the diffusion rate is increased compared to flooded electrodes in electrolytes.⁴

Table 5-Reliable aqueous media ENRR articles with high Faradaic efficiency (more than 20%)- All these works have a well performed ¹⁵N₂ experimental control that did the gas cleaning and repeated the experiments

No.	Catalyst	Electrolyte	FE%	Production rate (nmol s ⁻¹ cm ⁻²)	Experimental control scale	Ammonia production rate scale	Reliability indicator	year	Ref.
1	Fe-SAs/LCC/GC (Fe-O bond)	0.1 M KOH	51.0	2.51	25	2	50	2020	31
2	ECOF/BCP	0.1 M HCl	54.54	1.08	25	2	50	2021	35
3	B-COF/GO	10 M LiCl	71	0.95	25	2	50	2021	33
4	IVR-FO/GDY	0.1 M Na ₂ SO ₄	60.88	0.54	25	2	50	2021	36
5	WeSe ₂ -x	12 m LiClO ₄	62.5	0.59	25	2	50	2022	37
6	Fe/Co-O-C-1.0	0.1 M Na ₂ SO ₄	73.2	4.72	25	2	50	2022	38
7	Ag ₃ PO ₄	0.1 M KOH	26.67	7.23	25	2	50	2022	39

In terms of the catalyst two of these seven aqueous ENRR are metal-free catalysts (numbers 2, and 3 in Table 5).

In both of them, which were performed by Yan et al. group, the covalent organic framework-based materials (COF-based) were used as electrocatalyst.^{33,35} Covalent organic frameworks are extended crystalline organic materials with unique architectures, high surface areas, and tuneable pore sizes.⁴⁶ On the other hand, their relatively low conductivity, which yields low charge carrier mobility,⁴⁶ could account for their high FE in ENRR; according to Singh et al. discussion,⁹ limiting electron accessibility can improve NH₃ selectivity by suppressing the HER. It is worth to mention Zhao et al.⁴⁶ noticed that for COF-based HER catalysts, the so far presented electrocatalytic performances are still lower than those for Pt-based systems and many other non-noble metal HER catalysts due to their poor conductivity. Molecular dynamic (MD) simulation of diffusion process of the reactant combined with experiments performed by Yan et al. group demonstrated that exfoliated COF (ECOF) could facilitate the N₂ accessibility to catalyst and achieve high active and selective ENRR. The ECOF layer could suppress the HER by filtering out most of the active protons in the electrolyte due to the electrostatic interactions on the reaction interface. Furthermore, the strong van der Waals interactions

between COFs and nitrogen generate localized high N_2 concentration over the catalyst surface, which promotes the molecular collisions between N_2 and the active surface. By using this metal-free catalyst, a high Faradaic efficiency of 54.5% were achieved in an acidic solution.³⁵ In another work by Yan et al. group,³³ covalent organic frameworks with abundant boron sites were uniformly grown on graphene oxide nanosheet substrate to achieve great exposure of active sites (B-COF/GO). They also applied salting-out effect in a highly concentrated pH-neutral electrolyte solution, which not only reduces proton accessibility but also water activity, which could be beneficial for the selectivity of ENRR according to Singh et al.⁹. Indeed, highly concentrated LiCl (12 M) was suggested by MD simulation and verified by various in situ characterization, and finally confirmed by experiments results leading to a very high Faradaic efficiency of 71%.³³

Besides these two metal-free-based catalyst ENRR works, other works rely on metal-based catalysts. In two of them, which were performed by Zhao et al. group, the single atom catalysts (SACs) were used as electrocatalyst.^{31,38}. According to Skúlason and co-workers,⁴⁷ Fe, Mo, Ru, and Rh, are placed on top of the volcano plot and are the most active metals in ENRR. However, in ENRR under reducing conditions these surfaces are saturated by H adatoms instead of N, resulting in a much higher selectivity for a competing HER reaction. Structural modification and catalyst engineering could help to increase the ENRR selectivity of these metals. Since specific activity per metal atom increases with downsizing metal particles, the size of a metal catalyst is a key factor determining the catalytic performance. It is possible to achieve the ultimate specific activity with SACs, which contain atomically dispersed metal atoms in support materials.⁴⁸ Choi and co-workers⁴⁸ conducted DFT calculations on several SACs for ENRR. Specifically, they found that SACs exhibit a more positive free energy change of H adsorption ($\Delta G(*H)$) than most metal surfaces, suggesting that HER can be suppressed and the ENRR selectivity could be dramatically improved. Based on their discussion, the efficient reduction of nitrogen to ammonia via a high Faradaic efficiency of 51% and 73.2% of Zhao et al. group^{31,38} could result from applying Fe-based SAC as electrocatalyst. In their first work³¹, a coordination of Fe-(O-C₂)₄ as active sites supported on nitrogen-free lignocellulose-derived carbon was used as electrocatalyst, immobilized on a glassy carbon electrode. In the ENRR experiment, 0.1 M KOH at 12.7 pH as electrolyte helped NH₃ selectivity with more suppression of HER. In the other work³⁸, they used a synthesized bimetallic Fe-Co single-atom as electrocatalysts with a desired Fe/Co ratio and loading. Fe-

Co SAs were anchored on bacterial cellulose (BC)-derived graphitic carbon with the formation of $[(O-C_2)_3FeCo(O-C_2)_3]$ bonds. The Fe–Co SAC with the highest bimetallic active site density in a neutral electrolyte exhibited a very high Faradaic efficiency of 79% with a low overpotential of -0.3 V vs RHE.

Fang et al.³⁶ reported a facile and effective method to fabricate iron vacancy-rich ferroferric oxide on graphdiyne (IVR-FO/GDY), which the experimental and theoretical results showed that the GDY-induced iron vacancies in the catalyst activate the local O sites to transfer electrons towards graphdiyne to boost nitrogen reduction. Their cationic vacancy activation strategy resulted a high ammonia Faradaic efficiency of 60.88% at a positive potential of 0.26 V vs RHE. The other article that applied metal-based catalyst to implement ENRR was by Shen et al.³⁷. Combining catalyst and electrolyte engineering in this work led to a highly efficient electrochemical nitrogen reduction system with a promising Faradaic efficiency of 62.5%. The catalyst that was used in this work was WSe_{2-x} nanosheet which was obtained from WSe_2 nanosheet annealed under a mixed Ar/ H_2 atmosphere to create enriched Se vacancies verified by extensive characterizations. The free energy diagram of ENRR and HER on WSe_2 and WSe_{2-x} displayed that WSe_{2-x} exhibited a strong tendency for H_2O dissociation, which favoured the HER and retarded the ENRR; therefore, they adopted an electrolyte engineering strategy to suppress the HER by using water-in-salt electrolyte (WISE). To assess the role of electrolyte, they performed ENRR with WSe_{2-x} catalyst in two different electrolytes, diluted electrolyte (DE) 0.5 m $LiClO_4$ and WISE 12 m $LiClO_4$. The linear sweep voltammetry (LSV) curves of WSe_{2-x} in Ar and N_2 saturated DE and WISE showed that the current density difference between Ar and N_2 in WISE was larger than that in DE, which indicated that HER could be suppressed in WISE. Qualitative experiments also proved this by reaching high Faradaic efficiency of 62.5% in WISE compared to 11.8% in DE. Furthermore, the important role of catalyst engineering was experimentally proved by performing ENRR with WSe_2 in WISE, exhibiting 21.3% Faradaic efficiency, about three times lower than WSe_{2-x} . The last work of metal-based electrocatalysts was reported by Gupta et al.³⁹, which they modified metallic silver with inorganic phosphate to obtain silver phosphate Ag_3PO_4 catalyst. They applied a complexation-controlled synthetic approach for synthesis which resulted in an effective electrocatalyst for the ENRR in alkaline media under ambient conditions by exhibiting a high Faradaic efficiency of 26.67% at a positive potential of 0 V vs. RHE.

Interestingly, earlier theoretical studies reported ENRR potentials of around -0.6 V vs. RHE are needed to activate nitrogen, for best-performing metal catalysts, where these metals were found to bind hydrogen better than nitrogen, and thus found better to promote HER than ENRR.^{8,47} These calculated “activation” potentials are theoretical and are under zero current conditions and do not include any additional voltage drops (electrolyte, membrane, contact resistance, etc.). The catalysts discussed above reported to catalyze ENRR at potential ≥ 0 vs RHE; e.g. 0.26 V vs. RHE and 0 V vs. RHE, for IVR-FO/GDY³⁶ and Ag₃PO₄³⁹, respectively. This is significantly more positive than predicted by computational methods. Most of other successful approaches discussed above did not use ENRR potential more negative than -0.4 V vs. RHE (SI, Table S5). The ENRR field would greatly benefit if these successful approaches could be better understood from both theoretical and experimental perspectives. Possibly, the learnings made there could be translated to the electrochemical activation of other chemically stable molecules such as O₂ and CO₂, which occur at more negative potentials in aqueous media.

Energy efficiency of ENRR benchmarked against the Haber-Bosch Process

We further evaluated 98 reliable and probably reliable (aqueous + non-aqueous) works and compared them by energy efficiency, by relating the low heating value of ammonia and total electrical energy input to produce ammonia using ENRR. We state again the present analysis does not involve the energy cost to separate out clean, liquid anhydrous ammonia from water/organic solvent and to purify/compress the reaction gases. The energy cost we calculate is a lower bound (or a higher bound for energy efficiency).

Our analysis, as presented in Tables S5 and S6 and Fig. 3, showed that the reliable/probably reliable ENRR reports have a maximum energy efficiency of 55%, which is comparable to current Haber-Bosch ammonia plants, with seven of them practically relevant, as shown in Table 6, which are all aqueous media-based. Less than 15 percent of the reliable/probably reliable ENRR reports had energy efficiency between 20-35%. The others had less than 20% energy efficiency and need more improvements to be comparable with the Haber-Bosch process.

Table 6- ENRR articles with a practically relevant rated energy efficiency (more than 35%)- These two works among all aqueous and non- aqueous based media ENRR works are energy efficient ENRR, which both are aqueous based media

No.	Catalyst	Electrolyte	FE%	Potential (V vs RHE)	Production rate (nmol s ⁻¹ cm ⁻²)	Reliability indicator	Energy efficiency	Year	Ref.
1	B-COF/GO	10 M LiCl	71	-0.3	0.95	50	40.92	2021	33
2	IVR-FO/GDY	0.1 M Na ₂ SO ₄ 0.1 M PBS as	60.88	0.26	0.54	50	49.57	2021	36
3	Ru/CB NPs	catholyte/0.01 M H ₂ SO ₄ as anolyte	64.8	-0.1	0.99	20 ^b	41.74	2021	49
4	LiBi@VO-PTA	0.1 M Li ₂ SO ₄	85	-0.1	0.10	20	54.76	2021	50
5	Fe/Co-O-C-1.0	0.1 M Na ₂ SO ₄	73.2	-0.3	4.72	50	45.54	2022	38
6	Rh1/MnO ₂	9 m K ₂ SO ₄	73.3	-0.3	4.43 ^a	20	42.25	2022	51
7	Ag ₄ Ni ₂ NCs	0.1M HCl	78.97	-0.2	0.19	20 ^b	48.05	2022	52

^a The unit of yield rate is based on nmol s⁻¹mg⁻¹.

^b There are some works that have performed ¹⁵N₂ experiment qualitatively, done gas cleaning or even repeated the experiment. In this case, the experimental control scale is set to 10, as experiment that had proper gas cleaning and qualitative isotope nitrogen experiment is probably reliable.

As shown in Table 6, four of these practically relevant articles are probably reliable works with a reliability indicator of 20. Despite their promising efficiency, the ¹⁵N₂ control experiment was not repeated in none of these articles, also in articles Ref. 49 and Ref. 52 (raw 3 and 7 in Table 6, respectively) the ¹⁵N₂ control experiment was performed only qualitatively. The other three articles are those of the seven reliable aqueous based-media ENRR works with high Faradaic efficiency presented in Table 5 and explained from different points of view in the discussion above.^{33,36,38}

As shown in Fig. 4 and Table S6, the energy efficiency of non-aqueous media works, despite their high reliability and high production rates, were less than 20%, with a maximum of 15.1%. This was due to the high energy use to produce proton/electron sources (hydrogen/ethanol) but also due to the high cell potentials needed to keep Li-mediated ENRR running. In the SI (Section 6) we calculated the practically maximum attainable energy efficiency for ammonia production from H₂ as a proton/electron source using lithium mediated ENRR as an approach and obtained 24.2% based on *LHV*, provided low-grade waste heat cannot be reused in some other process. Approximately 1/3 of the energy cost in Li-mediated ENRR goes to the

proton/electron source and 2/3 to the electrochemical reactor, while in Haber-Bosch process the loop and the reactor consume very little energy, below 10%, while the largest energy consumption (90%) is on the side of hydrogen (proton/electron source) production. The high cell potential in Li-mediated ENRR was needed because Li seems to be consumed during the ENRR and needs to be constantly regenerated. Li is the most reductive metal and needs very negative potentials to be reduced/regenerated (-3.04 V vs. standard hydrogen electrode), which sets the minimum theoretical cell potential of Li regeneration at 3.04 V, not including any energy losses. Overall, the results in Fig. 3 and 4 show electrochemical synthesis of ammonia advanced significantly during the last few years, however improvements are needed in terms of energy efficiency and these technologies are yet to be verified at a higher technology readiness level.

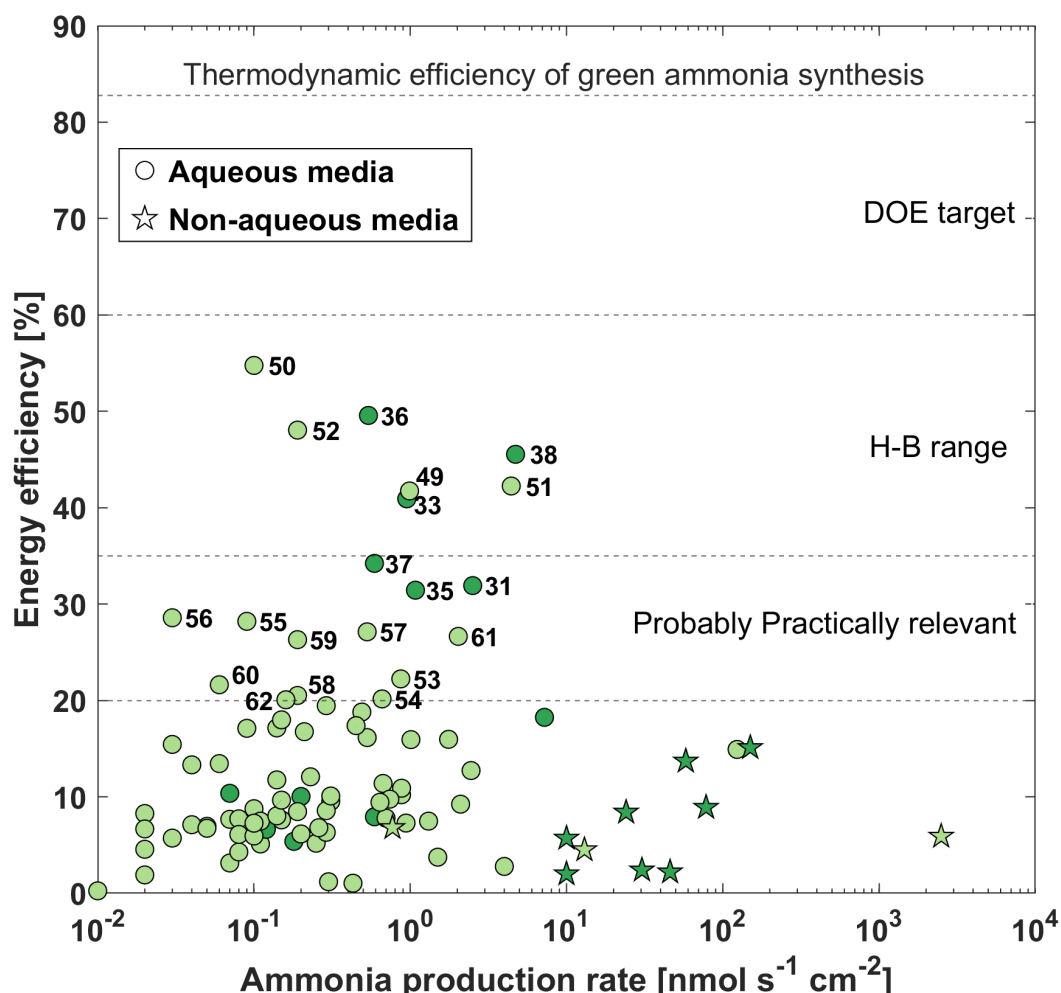


Figure 4- Energy efficiency of studies that were evaluated as probably reliable and reliable ^{31,33,35-38,49,50,52-62} – There are four intervals between the lines: below 20% line is interval 1 which the articles are not practically relevant however might find use in some niche markets, between line one and two (20-35%) is interval 2 that is probably practically relevant, between line

two and three (35-60%) represent interval 3 that are practically relevant, and above 60% is interval 4 that is goal for all processes including Haber-Bosch (H-B). The fourth line is the thermodynamic efficiency of green ammonia synthesis calculated based on the low heating value of ammonia. Colour codes are adopted from the Fig 1.

Conclusions

The evaluation of the non-aqueous works revealed that the most promising approach to achieve high selectivity and production rates of ammonia in electrochemical ammonia synthesis was: i) using electroplated Li metal at the cathode; ii) non-aqueous electrolyte with an optimal Li salt and proton concentration and iii) higher operating pressure of nitrogen (up to 20 bar).

Successful approaches in aqueous media involved highly selective catalyst materials, electrolytes with low concentrations of protons or lower activity of water molecules (water-in-salt electrolytes) and use of two compartment reactors separated by a membrane that favours the adsorption of nitrogen.

The evaluation of works in terms of their energy efficiency, reveals aqueous ENRR works can achieve energy efficiency of up to 55%, which makes them practically relevant. The energy efficiency of non-aqueous works is less than 15%, which makes them a less promising alternative to Haber-Bosch process. This was mainly related to very high cell potentials that are needed to constantly regenerate lithium metal, which ultimately increase the energy consumption of the electrochemical reactor.

Finally, during the last three years, a small percentage of published works were assessed reliable or probably reliable with the reliability indicator. This was mainly due to the low quality of control experiments and this needs to be improved in the future to help advance the state of the art faster.

Acknowledgement

This work was supported by. 1) Horizon 2020 project, Grant agreement 101022738, funded under SOCIETAL CHALLENGES - Secure, clean and efficient energy and 2) Independent Research Fund Denmark, case number 0217-00234B.

Author contributions

Conception by ED and FR.

Data collection FR.

Data analysis and interpretation by all.

Drafting the article by all.

Critical revision of the article by all.

Final approval of the version to be published by ED.

Data availability

Upon request to the corresponding author.

Competing interests

The authors declare no competing interests.

References

1. Lin, B., Wiesner, T. & Malmali, M. Performance of a Small-Scale Haber Process: A Techno-Economic Analysis. *ACS Sustain. Chem. Eng.* **8**, 15517–15531 (2020).
2. Rouwenhorst, K. H. R., Van der Ham, A. G. J., Mul, G. & Kersten, S. R. A. Islanded ammonia power systems: Technology review & conceptual process design. *Renew. Sustain. Energy Rev.* **114**, 109339 (2019).
3. Suryanto, B. H. R. *et al.* Nitrogen reduction to ammonia at high efficiency and rates based on a phosphonium proton shuttle. *Science* **372**, 1187–1191 (2021).
4. Lazouski, N., Chung, M., Williams, K., Gala, M. L. & Manthiram, K. Non-aqueous gas diffusion electrodes for rapid ammonia synthesis from nitrogen and water-splitting-derived hydrogen. *Nat. Catal.* **3**, 463–469 (2020).
5. Ravi, M. & Makepeace, J. W. Facilitating green ammonia manufacture under milder conditions: what do heterogeneous catalyst formulations have to offer? *Chem. Sci.* **13**, 890–908.
6. Suryanto, B. H. R. *et al.* Challenges and prospects in the catalysis of electroreduction of nitrogen to ammonia. *Nat. Catal.* **2**, 290–296 (2019).
7. Du, H.-L. *et al.* Electroreduction of nitrogen at almost 100% current-to-ammonia efficiency. *Nature* (2022) doi:10.1038/s41586-022-05108-y.
8. Dražević, E. & Skúlason, E. Are There Any Overlooked Catalysts for Electrochemical NH₃ Synthesis—New Insights from Analysis of Thermochemical Data. *iScience* **23**, 101803 (2020).

9. Singh, A. R. *et al.* Electrochemical Ammonia Synthesis—The Selectivity Challenge. *ACS Catal.* **7**, 706–709 (2017).
10. Andersen, S. Z. *et al.* A rigorous electrochemical ammonia synthesis protocol with quantitative isotope measurements. *Nature* **570**, 504–508 (2019).
11. Choi, J. *et al.* Electroreduction of Nitrates, Nitrites, and Gaseous Nitrogen Oxides: A Potential Source of Ammonia in Dinitrogen Reduction Studies. *ACS Energy Lett.* **5**, 2095–2097 (2020).
12. Li, L., Tang, C., Yao, D., Zheng, Y. & Qiao, S.-Z. Electrochemical Nitrogen Reduction: Identification and Elimination of Contamination in Electrolyte. *ACS Energy Lett.* **4**, 2111–2116 (2019).
13. MacLaughlin, C. Role for Standardization in Electrocatalytic Ammonia Synthesis: A Conversation with Leo Liu, Lauren Greenlee, and Douglas MacFarlane. *ACS Energy Lett.* **4**, 1432–1436 (2019).
14. Choi, J. *et al.* Identification and elimination of false positives in electrochemical nitrogen reduction studies. *Nat. Commun.* **11**, 5546 (2020).
15. Giddey, S., Badwal, S. P. S. & Kulkarni, A. Review of electrochemical ammonia production technologies and materials. *Int. J. Hydrog. Energy* **38**, 14576–14594 (2013).
16. Martín, A. J., Shinagawa, T. & Pérez-Ramírez, J. Electrocatalytic Reduction of Nitrogen: From Haber-Bosch to Ammonia Artificial Leaf. *Chem* **5**, 263–283 (2019).
17. Informatics, N. O. of D. and. NIST Chemistry WebBook. <https://webbook.nist.gov/chemistry/doi:10.18434/T4D303>.
18. Mukouyama, Y., Iida, K. & Kuge, T. Electrooxidation of Ethanol on Pt in the Absence of Water. *Electrochemistry* **88**, 178–184 (2020).
19. Durst, J., Simon, C., Hasché, F. & Gasteiger, H. A. Hydrogen Oxidation and Evolution Reaction Kinetics on Carbon Supported Pt, Ir, Rh, and Pd Electrocatalysts in Acidic Media. *J. Electrochem. Soc.* **162**, F190 (2014).
20. Smith, C., K. Hill, A. & Torrente-Murciano, L. Current and future role of Haber–Bosch ammonia in a carbon-free energy landscape. *Energy Environ. Sci.* **13**, 331–344 (2020).

21. Morgan, E. R., Manwell, J. F. & McGowan, J. G. Sustainable Ammonia Production from U.S. Offshore Wind Farms: A Techno-Economic Review. *ACS Sustain. Chem. Eng.* **5**, 9554–9567 (2017).
22. Izelaar, B. *et al.* Revisiting the Electrochemical Nitrogen Reduction on Molybdenum and Iron Carbides: Promising Catalysts or False Positives? *ACS Catal.* 1649–1661 (2023) doi:10.1021/acscatal.2c04491.
23. Liu, Y. *et al.* Engineering Mo/Mo₂C/MoC hetero-interfaces for enhanced electrocatalytic nitrogen reduction. *J. Mater. Chem. A* **8**, 8920–8926 (2020).
24. Qin, B. *et al.* Understanding of nitrogen fixation electro catalyzed by molybdenum–iron carbide through the experiment and theory. *Nano Energy* **68**, 104374 (2020).
25. Hanifpour, F. *et al.* Investigation into the mechanism of electrochemical nitrogen reduction reaction to ammonia using niobium oxynitride thin-film catalysts. *Electrochimica Acta* **403**, 139551 (2022).
26. Wang, X., Huang, J., Hu, F., Chen, J. & Yao, X. Synthesis of B-doped C₃N₄ nanosheets by secondary sintering for enhanced electrocatalytic nitrogen fixation performance. *J. Nanoparticle Res.* **23**, 63 (2021).
27. Li, K. *et al.* Enhancement of lithium-mediated ammonia synthesis by addition of oxygen. *Science* **374**, 1593–1597 (2021).
28. Cai, X. *et al.* Lithium-mediated electrochemical nitrogen reduction: Mechanistic insights to enhance performance. *iScience* **24**, 103105 (2021).
29. Fu, Y. *et al.* Dual-metal-driven Selective Pathway of Nitrogen Reduction in Orderly Atomic-hybridized Re₂MnS₆ Ultrathin Nanosheets. *Nano Lett.* **20**, 4960–4967 (2020).
30. Chu, K. *et al.* Multi-functional Mo-doping in MnO₂ nanoflowers toward efficient and robust electrocatalytic nitrogen fixation. *Appl. Catal. B Environ.* **264**, 118525 (2020).
31. Zhang, S. *et al.* Electrocatalytically Active Fe-(O-C₂)₄ Single-Atom Sites for Efficient Reduction of Nitrogen to Ammonia. *Angew. Chem. Int. Ed.* **59**, 13423–13429 (2020).

32. Yuan, M. *et al.* Support effect boosting the electrocatalytic N₂ reduction activity of Ni₂P/N,P-codoped carbon nanosheet hybrids. *J. Mater. Chem. A* **8**, 2691–2700 (2020).
33. Wang, M. *et al.* Salting-out effect promoting highly efficient ambient ammonia synthesis. *Nat. Commun.* **12**, 3198 (2021).
34. Lv, X.-W., Liu, X.-L., Suo, Y.-J., Liu, Y.-P. & Yuan, Z.-Y. Identifying the Dominant Role of Pyridinic-N–Mo Bonding in Synergistic Electrocatalysis for Ambient Nitrogen Reduction. *ACS Nano* **15**, 12109–12118 (2021).
35. Liu, S. *et al.* Proton-filtering covalent organic frameworks with superior nitrogen penetration flux promote ambient ammonia synthesis. *Nat. Catal.* **4**, 322–331 (2021).
36. Fang, Y. *et al.* Graphdiyne-Induced Iron Vacancy for Efficient Nitrogen Conversion. *Adv. Sci.* **9**, 2102721 (2022).
37. Shen, P. *et al.* High-Efficiency N₂ Electroreduction Enabled by Se-Vacancy-Rich WSe_{2-x} in Water-in-Salt Electrolytes. *ACS Nano* (2022) doi:10.1021/acsnano.2c00596.
38. Zhang, S. *et al.* Atomically dispersed bimetallic Fe–Co electrocatalysts for green production of ammonia. *Nat. Sustain.* 1–11 (2022) doi:10.1038/s41893-022-00993-7.
39. Gupta, D. *et al.* High yield selective electrochemical conversion of N₂ to NH₃ via morphology controlled silver phosphate under ambient conditions. *J. Mater. Chem. A* **10**, 20616–20625 (2022).
40. Tian, Y. *et al.* Magnetron sputtering tuned “ π back-donation” sites over metal oxides for enhanced electrocatalytic nitrogen reduction. *J. Mater. Chem. A* **10**, 2800–2806 (2022).
41. Andersen, S. Z. *et al.* Increasing stability, efficiency, and fundamental understanding of lithium-mediated electrochemical nitrogen reduction. *Energy Environ. Sci.* **13**, 4291–4300 (2020).
42. Schwalbe, J. A. *et al.* A Combined Theory-Experiment Analysis of the Surface Species in Lithium-Mediated NH₃ Electrosynthesis. *ChemElectroChem* **7**, 1542–1549 (2020).
43. Li, K. *et al.* Increasing Current Density of Li-Mediated Ammonia Synthesis with High Surface Area Copper Electrodes. *ACS Energy Lett.* **7**, 36–41 (2022).

44. Zhao, R. *et al.* Recent progress in the electrochemical ammonia synthesis under ambient conditions. *EnergyChem* **1**, 100011 (2019).
45. Chalkley, M. J., Del Castillo, T. J., Matson, B. D. & Peters, J. C. Fe-Mediated Nitrogen Fixation with a Metallocene Mediator: Exploring pKa Effects and Demonstrating Electrocatalysis. *J. Am. Chem. Soc.* **140**, 6122–6129 (2018).
46. Zhao, X., Pachfule, P. & Thomas, A. Covalent organic frameworks (COFs) for electrochemical applications. *Chem. Soc. Rev.* **50**, 6871–6913 (2021).
47. Skúlason, E. *et al.* A theoretical evaluation of possible transition metal electro-catalysts for N₂ reduction. *Phys. Chem. Chem. Phys.* **14**, 1235–1245 (2011).
48. Choi, C. *et al.* Suppression of Hydrogen Evolution Reaction in Electrochemical N₂ Reduction Using Single-Atom Catalysts: A Computational Guideline. *ACS Catal.* **8**, 7517–7525 (2018).
49. Wei, X., Pu, M., Jin, Y. & Wessling, M. Efficient Electrocatalytic N₂ Reduction on Three-Phase Interface Coupled in a Three-Compartment Flow Reactor for the Ambient NH₃ Synthesis. *ACS Appl. Mater. Interfaces* **13**, 21411–21425 (2021).
50. Liao, W. *et al.* Lithium/bismuth co-functionalized phosphotungstic acid catalyst for promoting dinitrogen electroreduction with high Faradaic efficiency. *Cell Rep. Phys. Sci.* **2**, 100557 (2021).
51. Shen, P. *et al.* Ultra-efficient N₂ electroreduction achieved over a rhodium single-atom catalyst (Rh₁/MnO₂) in water-in-salt electrolyte. *Appl. Catal. B Environ.* **316**, 121651 (2022).
52. Han, M. *et al.* Effect of Heteroatom and Charge Reconstruction in Atomically Precise Metal Nanoclusters on Electrochemical Synthesis of Ammonia. *Adv. Funct. Mater.* **32**, 2202820 (2022).
53. Yang, H. *et al.* Achieving High Activity and Selectivity of Nitrogen Reduction via Fe–N₃ Coordination on Iron Single-Atom Electrocatalysts at Ambient Conditions. *ACS Sustain. Chem. Eng.* **8**, 12809–12816 (2020).
54. Zhang, J. *et al.* Three-Phase Electrolysis by Gold Nanoparticle on Hydrophobic Interface for Enhanced Electrochemical Nitrogen Reduction Reaction. *Adv. Sci.* **7**, 2002630 (2020).

55. Nazemi, M., Soule, L., Liu, M. & El-Sayed, M. A. Ambient Ammonia Electrosynthesis from Nitrogen and Water by Incorporating Palladium in Bimetallic Gold–Silver Nanocages. *J. Electrochem. Soc.* **167**, 054511 (2020).
56. Chen, J. *et al.* The activation of porous atomic layered MoS₂ basal-plane to induce adjacent Mo atom pairs promoting high efficiency electrochemical N₂ fixation. *Appl. Catal. B Environ.* **285**, 119810 (2021).
57. Wang, Z. *et al.* Phosphorus modulation of a mesoporous rhodium film for enhanced nitrogen electroreduction. *Nanoscale* **13**, 13809–13815 (2021).
58. Wang, C. *et al.* Hierarchical CoS₂/MoS₂ flower-like heterostructured arrays derived from polyoxometalates for efficient electrocatalytic nitrogen reduction under ambient conditions. *J. Colloid Interface Sci.* **609**, 815–824 (2022).
59. Guo, Y. *et al.* Regulating nitrogenous adsorption and desorption on Pd clusters by the acetylene linkages of hydrogen substituted graphdiyne for efficient electrocatalytic ammonia synthesis. *Nano Energy* **86**, 106099 (2021).
60. Ma, X., Zhang, Q., Gao, L., Zhang, Y. & Hu, C. Atomic-layer-deposited oxygen-deficient TiO₂ on carbon cloth: an efficient electrocatalyst for nitrogen fixation. *ChemCatChem* **n/a**,.
61. Zhang, S. *et al.* Ambient Electrochemical Nitrogen Fixation over a Bifunctional Mo–(O–C₂)₄ Site Catalyst. *J. Phys. Chem. C* **126**, 965–973 (2022).
62. Li, C., Wang, M., Ren, L. & Sun, H. Promoting the formation of oxygen vacancies in ceria multishelled hollow microspheres by doping iron for enhanced ambient ammonia electrosynthesis. *Inorg. Chem. Front.* **9**, 1467–1473 (2022).